

# Mass distribution in the quasi-mono-energetic neutron-induced fission of $^{232}\text{Th}$

H. Naik<sup>1,a</sup>, Rita Crasta<sup>2</sup>, S.V. Suryanarayana<sup>3</sup>, P.M. Prajapati<sup>4</sup>, V.K. Mulik<sup>5</sup>, B.S. Shivasankar<sup>6</sup>, K.C. Jagadeesan<sup>7</sup>, S.V. Thakare<sup>7</sup>, S.C. Sharma<sup>3</sup>, and A. Goswami<sup>1</sup>

<sup>1</sup> Radiochemistry Division, Bhabha Atomic Research Centre, Mumbai - 400 085, India

<sup>2</sup> Microtron Centre, Department of Studies in Physics, Mangalore University, Mangalagangothri-574 199, Karnataka, India

<sup>3</sup> Nuclear Physics Division, Bhabha Atomic Research Centre, Mumbai - 400 085, India

<sup>4</sup> Physics Department, Faculty of Science, The M. S. University of Baroda, Vadodara - 390 002, India

<sup>5</sup> Department of Physics, University of Pune - 411 007, India

<sup>6</sup> Department of Statistics, Manipal University, Manipal - 576 104, India

<sup>7</sup> Radiopharmaceutical Division, Bhabha Atomic Research Centre, Mumbai - 400 085, India

Received: 29 June 2014 / Revised: 10 August 2014

Published online: 19 September 2014 – © Società Italiana di Fisica / Springer-Verlag 2014

Communicated by H. Miyatake

**Abstract.** The cumulative yields of various fission products in  $^{232}\text{Th}(n, f)$  with average neutron energies of 6.35, 8.53 and 10.09 MeV have been determined using an off-line  $\gamma$ -ray spectrometric technique. The neutron beam was produced from the  $^7\text{Li}(p, n)$  reaction. From the cumulative fission yields, the mass chain yields were obtained by using charge distribution correction of medium energy. The peak-to-valley ( $P/V$ ) ratio, the average value of light mass ( $\langle A_L \rangle$ ), heavy mass ( $\langle A_H \rangle$ ) and the average number of neutrons ( $\langle \nu \rangle$ ) at the three different neutron energies of the present work and at other energies from the literature in the  $^{232}\text{Th}(n, f)$  reaction were obtained from the mass yield data. The present and the existing literature data in the  $^{232}\text{Th}(n, f)$  reaction at various excitation energies were compared with similar data in the  $^{238}\text{U}(n, f)$  reaction. The fine structure in the mass yield distribution was interpreted from the point of nuclear structure effect such as shell closure proximity and even-odd effect. The role of standard I and standard II asymmetric mode of fission was discussed. The different types of mass-yield distributions between  $^{232}\text{Th}(n, f)$  and  $^{238}\text{U}(n, f)$  reactions were explained from different types of the potential energy between the two fissioning systems. The role of excitation energy was also investigated.

## 1 Introduction

Measurements of nuclear data such as neutron capture cross-sections, fission cross-sections and fission yields are required for many reactor calculations. Sufficient data on neutron capture cross-section and fission cross-section over a wide range of neutron energies from thermal to MeV range are available in the literature [1–3]. Similarly, the fission yields data in the neutron-induced fission of actinides, ranging from  $^{227}\text{Th}$  to  $^{257}\text{Fm}$ , are available from different compilations [4–8]. Among the nuclear data, the fission yields in the neutron-induced fission of the isotopes of actinides, ranging from Th to Cm are important for their applications in conventional light- and heavy-water reactors as well as fast reactors [9–13], advanced heavy-water reactors (AHWR) [14,15] and accelerator-driven subcritical systems (ADSs) [16–21].

Besides the above applications, basic studies in the fission yield distribution in the low-energy fission of actinides

provide important information about the nuclear structure effect (*e.g.*, shell closure proximity and even-odd effect) and descent dynamics from the point of saddle to scission [2,3]. It is a well-known fact that the mass yield distributions in the spontaneous and neutron-induced fission of heavy- $Z$  actinides (*e.g.*, Es to Lr) are symmetric in nature [2,3]. On the other hand, the mass yield distributions in the neutron-induced fission of medium- $Z$  actinides (*e.g.*, U to Cf) are asymmetric with double hump, whereas for light- $Z$  actinides (*e.g.*, Ac, Th, Pa) are asymmetric with triple hump [2,3]. Other than this, the fine structures due to the even-odd effect and shell closure proximity have been observed in the low-energy neutron-induced fission of light and medium even- $Z$  actinides. This was also seen for the fission fragments yield data of neutron-deficient lighter even- $Z$  actinides such as  $^{220-229}\text{Th}$  and  $^{231-234}\text{U}$  in the excitation energy range of the GDR region due to electromagnetic fission in inverse kinematics [22–24]. Similarly, the nuclear structure effect in the reactor [25–28] and mono-energetic [29–82] neutron-induced fissions of  $^{232}\text{Th}$  and  $^{238}\text{U}$  can be seen. The fission yield data in the

<sup>a</sup> e-mail: [naikhbarc@yahoo.com](mailto:naikhbarc@yahoo.com)

mono-energetic neutron-induced fission of  $^{238}\text{U}$  are available in the literature [54–82], within the neutron energy of 1.5 to 17.7 MeV. However, systematic fission yield data in the mono-energetic neutron-induced fission of  $^{232}\text{Th}$  are available in the literature [29–52], only within the neutron energy of 2 to 8 MeV and at 14.8 MeV. Within the neutron energy of 8 to 14.8 MeV, sufficient fission yield data for  $^{232}\text{Th}(n, f)$  are not available in the literature to examine the effect of nuclear structure. At higher neutron energies, the experimental results in the 33–60 MeV quasi-mono-energetic neutron-induced fission of  $^{232}\text{Th}$  and  $^{238}\text{U}$  are available from physical measurements [53], where the effect of the nuclear structure is not expected. In view of this, in the present work, the yields of various fission products in the  $^{232}\text{Th}(n, f)$ , with average neutron energies of 6.35, 8.53 and 10.09 MeV, have been determined using an off-line  $\gamma$ -ray spectrometric technique. From the yields of the fission products, their mass chain yields were obtained by using charge distribution correction [8, 83]. The fission product yields data in the three neutron energies of the present work and at other neutron energies from the literature [29–52] in  $^{232}\text{Th}(n, f)$  are compared with similar data in  $^{238}\text{U}(n, f)$  [52–82] to examine the role of the excitation energy in the nuclear structure effect. The role of the excitation energy in the peak-to-valley ( $P/V$ ) ratio was examined. The variation of average light ( $\langle A_L \rangle$ ) and heavy ( $\langle A_H \rangle$ ) masses as well the average neutron number ( $\langle \nu \rangle$ ) as a function of the excitation energy has been also discussed.

## 2 Experimental details

The quasi-mono-energetic neutron beam used in the present experiment was obtained from the  $^7\text{Li}(p, n)^7\text{Be}$  reaction by using the proton beam from the 14UD BARC-TIFR Pelletron facility at Mumbai, India [84, 85]. A collimator of 6 mm diameter was used before the Li target to avoid the energy spread of the proton beam. The lithium foil used was made up of natural lithium with thickness of 3.7 mg/cm<sup>2</sup>, sandwiched between two tantalum foils of different thickness. The front tantalum foil facing the proton beam is 3.9 mg/cm<sup>2</sup> thick, in which the degradation of proton energy is only 50–80 keV [86]. On the other hand, the back tantalum foil is 0.025–0.1 mm thick, which is sufficient to stop the proton beam. Behind the Ta-Li-Ta stack, the  $^{232}\text{Th}$  metal foil wrapped with a 0.025 mm thick super pure aluminum foil was used for irradiation. The aluminum wrapper was used as a catcher foil to stop fission products recoiling out from the  $^{232}\text{Th}$  metal foil during the irradiation. The size of each  $^{232}\text{Th}$  metal foil was about 1.0 cm<sup>2</sup> with thickness of about 323.7–325.2 mg/cm<sup>2</sup>. The sample was mounted at zero degree angle in the forward direction with respect to the beam direction at a distance of 2.1 cm from the location of the Ta-Li-Ta stack. Different sets of Ta-Li-Ta stacks and Al-wrapped  $^{232}\text{Th}$  samples were made for different irradiations at various neutron energies. The sample was then irradiated by neutrons generated by impinging the proton beam on the lithium metal foil through the thin tantalum foil of the Ta-Li-Ta metal

stack. The irradiations time were for 5–15 h depending upon the proton energy faced by the front tantalum foil. The proton energies used in the present work were 10, 14 and 18 MeV, respectively. The proton current during the irradiations varied within 200 to 400 nA. The corresponding maximum energies of the neutron beam impinging on the  $^{232}\text{Th}$  samples were 8.12, 12.12 and 16.12 MeV, respectively. After each irradiation, the samples were cooled for 2–3 h.

The irradiated  $^{232}\text{Th}$  targets along with aluminum catcher were mounted on different Perspex plates. The  $\gamma$ -rays counting of the fission products from the irradiated samples were done in a energy- and efficiency-calibrated 80 cm<sup>3</sup> HPGe detector coupled to a PC-based 4K channel analyzer. The dead time of counting was always less than 5% by placing the irradiated sample at a suitable distance from the end cap of the detector to avoid pile-up effects. The  $\gamma$ -ray counting of the sample was done in live-time mode and was followed as a function of time. The resolution of the detector system during counting was 1.8 keV FWHM at 1332.5 keV of  $^{60}\text{Co}$ . The energy and efficiency calibration of the detector system was performed by using the 121.8 to 1408.01 keV  $\gamma$ -rays from standard  $^{152}\text{Eu}$  source at same geometry, where the summation error was negligible. This was checked by comparing the efficiency obtained from  $\gamma$ -ray counting of standards such as  $^{241}\text{Am}$  (59.5 keV),  $^{133}\text{Ba}$  (80.9, 276.4, 302.9, 356.0, and 383.8 keV),  $^{137}\text{Cs}$  (661.7 keV),  $^{54}\text{Mn}$  (834.6 keV),  $^{60}\text{Co}$  (1173 and 1332 keV). The detector efficiency was 20% at 1332.5 keV, relative to 3" diameter  $\times$  3" length NaI(Tl) detector. The uncertainty in the efficiency was 2–3%. For each irradiated samples, several sets of measurements were done with increasing counting time to cover the different fission products, from the half-life of 50 minutes to 33 days. The  $\gamma$ -ray counting of the irradiated  $^{232}\text{Th}$  samples was done up to few months to check the half-life of the fission products of interest.

## 3 Calculation and results

### 3.1 Calculation of the neutron energy

The neutron flux in the present experiment were produced from the  $^7\text{Li}(p, n)$  reaction [87–89] of the natural occurring  $^7\text{Li}$  with isotopic abundance of 92.41%. The  $Q$ -value for the  $^7\text{Li}(p, n)^7\text{Be}$  reaction to the ground state is  $-1.644$  MeV, whereas the first excited state is 0.431 MeV above ground state leading to an average  $Q$ -value of  $-1.868$  MeV. However, the threshold value to populate the ground state of  $^7\text{Be}$  is 1.881 MeV. Thus, for the proton energies of 10, 14 and 18 MeV, the resulting peak energies of first group of neutrons ( $n_0$ ) will be 8.12, 12.12 and 16.12 MeV, respectively. The corresponding neutron energies of second group of neutrons ( $n_1$ ), for the first excited state of  $^7\text{Be}$  will be 7.63, 11.63 and 15.63 MeV, respectively. This is because, above 2.37 MeV, the  $n_1$  group of neutron is also produced. Above the proton energy of 4.5 MeV, the fragmentation of  $^8\text{Be}$  to  $^4\text{He} + ^3\text{He} + n$  ( $Q = -3.23$  MeV) takes place, which causes continuous

neutron energy distribution besides  $n_0$  and  $n_1$  groups of neutrons. Meadows and Smith [88] have given experimental neutron distributions from the break-up channels and also parameterized these distributions. We have generated the neutron spectrum using the neutron energy distribution given by C.H. Poppe *et al.* [89] and shown in our earlier work [84, 85]. From those neutron spectrums [84, 85], the flux-weighted average neutron energies were calculated as 6.35, 8.53 and 10.09 MeV, respectively. The energy spread for the above average neutron energies range from around 0.3 to 0.7 MeV [84, 85].

### 3.2 Calculation of fission product yields

The numbers of detected ( $N_{\text{obs}}$ )  $\gamma$ -rays for the fission products of interest were obtained by subtracting the linear Compton background from the total peak areas. From  $N_{\text{obs}}$  of an individual fission product, the cumulative yields ( $Y_{\text{R}}$ ) relative to  $^{92}\text{Sr}$  were calculated by using the usual decay equation [27, 28],

$$Y_{\text{R}} = \frac{N_{\text{obs}}(\text{CL}/\text{LT})\lambda}{n\sigma_f\varphi I_\gamma \varepsilon(1 - e^{-\lambda t})e^{-\lambda T}(1 - e^{-\lambda \text{CL}})}, \quad (1)$$

where  $n$  is the number of target atoms,  $\varphi$  is the neutron flux and  $\sigma_f$  is the neutron fluxed average fission cross-section of  $^{232}\text{Th}$  at 6.35, 8.53 and 10.09 MeV.  $I_\gamma$  is the  $\gamma$ -ray intensity or  $\gamma$ -ray emission probability,  $\varepsilon$  is the detection efficiency of the  $\gamma$ -rays in the detector system and  $\lambda$  is the decay constant of the fission-product of interest ( $\lambda = \ln 2/T_{1/2}$ ).  $t$  and  $T$  are the irradiation and cooling times, whereas, CL and LT are the real time and the live time of counting, respectively.

From eq. (1), the  $n\sigma_f\varphi$  term was first obtained from the photo-peak activity of 1383.9 keV  $\gamma$ -line and by assuming the cumulative yield ( $Y_{\text{R}}$ ) of  $^{92}\text{Sr}$  as 1.0. Thus the individual terms, such as  $n$ ,  $\sigma_f$  and  $\varphi$ , are not necessary to be used separately. The nuclear spectroscopic data, such as the  $\gamma$ -ray energies, the half-lives ( $T_{1/2}$ ), and the  $\gamma$ -ray intensity ( $I_\gamma$ ) of the fission products were taken from the literature [90, 91]. Then, by using the  $n\sigma_f\varphi$  term in eq. (1), the relative cumulative yields ( $Y_{\text{R}}$ ) of other fission products were obtained from the photo-peak activities of the  $\gamma$ -lines of corresponding fission products. From the  $Y_{\text{R}}$  values of the fission products, their relative mass-chain yields ( $Y_{\text{RA}}$ ) were calculated after correcting for charge distribution [8, 83]. According to Wahl's prescription [8], the fractional cumulative yield ( $Y_{\text{FCY}}$ ) of a fission product in an isobaric mass chain is given as

$$Y_{\text{FCY}} = \frac{\text{EOF}^{a(Z)}}{\sqrt{2\pi\sigma^2}} \int_{-\infty}^{Z+0.5} \exp[-(Z - Z_{\text{P}})^2/2\sigma^2] dZ, \quad (2)$$

$$Y_{\text{RA}} = Y_{\text{R}}/Y_{\text{FCY}}, \quad (3)$$

where  $Z_{\text{P}}$  is the most probable charge and  $\sigma_z$  is the width parameter of an isobaric-yield distribution.  $\text{EOF}^{a(Z)}$  is the even-odd effect with  $a(Z) = +1$  for even- $Z$  nuclides and  $-1$  for odd- $Z$  nuclides.

From the above equations it can be seen that in an isobaric mass chain, it is necessary to have knowledge of  $Z_{\text{P}}$ ,  $\sigma_z$  and  $\text{EOF}^{a(Z)}$  to calculate the  $Y_{\text{FCY}}$  value of a fission product and thus the mass-chain yield ( $Y_{\text{RA}}$ ). The  $\text{EOF}^{a(Z)}$  values in the medium-energy fission is negligible. It was shown by Umezawa *et al.* [83] that the  $\sigma_z$  value in medium-energy proton- and alpha-induced fission of  $^{232}\text{Th}$  and  $^{238}\text{U}$  is  $0.70 \pm 0.06$ . The  $Z_{\text{P}}$  values of the individual mass chain ( $A$ ) in the neutron-induced fission of  $^{232}\text{Th}$  at the average energy of 6.35, 8.53 and 10.09 MeV were calculated based on the prescription of Umezawa *et al.* [83] as

$$Z_{\text{P}} = \eta Z_{\text{F}} \pm \Delta Z_{\text{P}}, \quad \eta Z_{\text{F}} = Z_{\text{UCD}} = (Z_{\text{F}}/A_{\text{F}})(A + v_{\text{post}}), \quad (4a)$$

$$\eta = (A + v_{\text{post}})/(A_{\text{C}} - v_{\text{pre}}), \quad A_{\text{F}} = A_{\text{C}} - v_{\text{pre}}, \quad (4b)$$

where  $Z_{\text{C}}$  and  $A_{\text{C}}$  are the charge and mass of the compound nucleus.  $Z_{\text{F}}$  and  $A_{\text{F}}$  are the charge and mass of the fissioning system ( $^{233}\text{Th}^*$ ).  $Z_{\text{UCD}}$  is the most probable charge based on the unchanged charge-density distribution as suggested by Sugarman and Turkevich [92].  $A$  is the mass of the fission product and  $\Delta Z_{\text{P}}$  ( $= Z_{\text{P}} - Z_{\text{UCD}}$ ) is the charge-polarization parameter. The  $+$  and  $-$  signs for the  $\Delta Z_{\text{P}}$  value are applicable to light and heavy fragments, respectively.  $v_{\text{pre}}$  and  $v_{\text{post}}$  are pre- and post-fission neutrons at scission, which were calculated from the excitation energy ( $E^*$ ) of the compound nucleus using the following relations [83]:

$$v_{\text{pre}} = \frac{E^*}{7.5 \pm 0.5} + \frac{Z_{\text{C}}}{2A_{\text{C}}} - (19.0 \pm 0.5), \quad 1.0 \text{ for } A > 88, \quad (5a)$$

$$v_{\text{post}} = 1.0 \text{ for } A > 88, 1.0 + 0.1(A - 88) \text{ for } 78 < A < 88, \\ 0 \text{ for } A < 78. \quad (5b)$$

For the average neutron energies of 6.35, 8.53 and 10.09 MeV, the excitation energy ( $E^*$ ) of the compound nucleus is 10.96, 13.14 and 14.7 MeV, respectively. The  $E^*$  values were used in eq. (5b) to calculate the  $v_{\text{pre}}$  values at three different neutron energies. The  $v_{\text{pre}}$  and  $v_{\text{post}}$  values obtained from eqs. (5b) and (5b) were used in eqs. (4a) and (4b) to calculate the value of  $Z_{\text{UCD}}$  as a function of mass number for the different fission products. The  $\Delta Z_{\text{P}}$  value was then calculated from the following relation [83]:

$$\Delta Z_{\text{P}} = 0, \text{ for } I\eta - 0.5I < 0.04, \quad (6a)$$

$$\Delta Z_{\text{P}} = (20/3)(I\eta - 0.5I - 0.04), \\ \text{for } 0.04 < I\eta - 0.5I < 0.085. \quad (6b)$$

The  $Z_{\text{P}}$  value as a function of mass number and the average width parameter ( $\sigma_z$ ) of 0.7 were used in eq. (2) to obtain the  $Y_{\text{FCY}}$  values for individual fission products. The relative mass-chain yield ( $Y_{\text{RA}}$ ) of the fission products from their relative cumulative yield ( $Y_{\text{R}}$ ) were obtained in eq. (3) by using the  $Y_{\text{FCY}}$  values of different fission products. The relative mass-chain yields ( $Y_{\text{RA}}$ ) of the fission products obtained were then normalized to a total yield of 200% to calculate the absolute mass-chain yields ( $Y_{\text{A}}$ ).

**Table 1.** Nuclear spectroscopic data and yields of fission products in the 6.35, 8.53 and 10.09 MeV neutron-induced fission of  $^{232}\text{Th}$ .  $Y_{\text{R}}$  – Cumulative yields;  $Y_{\text{A}}$  – Mass yields;  $^{92}\text{Sr}$  – Fission rate monitor.

Nuclide	Half-life	$\gamma$ -ray energy (keV)	$\gamma$ -ray intensity (%)	6.35 MeV $Y_{\text{C}}$ (%)	6.35 MeV $Y_{\text{A}}$ (%)	8.53 MeV $Y_{\text{C}}$ (%)	8.53 MeV $Y_{\text{A}}$ (%)	10.09 MeV $Y_{\text{C}}$ (%)	10.09 MeV $Y_{\text{A}}$ (%)
$^{85}\text{Kr}^{\text{m}}$	4.48 h	151.2	$75.0 \pm 0.4$	$3.870 \pm 0.304$	$3.870 \pm 0.304$	$2.956 \pm 0.297$	$2.956 \pm 0.297$	$3.225 \pm 0.082$	$3.225 \pm 0.082$
		304.9	$14.0 \pm 0.5$	$3.846 \pm 0.375$	$3.846 \pm 0.375$	$2.919 \pm 0.343$	$2.919 \pm 0.343$	$3.571 \pm 0.177$	$3.571 \pm 0.177$
$^{87}\text{Kr}$	76.3 min	402.6	$49.6 \pm 2.0$	$5.970 \pm 0.710$	$5.988 \pm 0.712$	$5.970 \pm 0.710$	$5.988 \pm 0.712$	$5.864 \pm 0.268$	$5.882 \pm 0.273$
$^{88}\text{Kr}$	2.84 h	196.3	$25.98 \pm 1.7$	$5.336 \pm 0.126$	$5.423 \pm 0.128$	$5.336 \pm 0.126$	$5.423 \pm 0.128$	$5.268 \pm 0.268$	$5.354 \pm 0.273$
$^{91}\text{Sr}$	9.63 h	749.8	$23.61 \pm 1.7$	$6.268 \pm 0.556$	$6.268 \pm 0.556$	$5.621 \pm 0.449$	$5.621 \pm 0.449$	$5.577 \pm 0.610$	$5.577 \pm 0.610$
		1024.3	$33.0 \pm 0.7$	$6.202 \pm 0.617$	$6.202 \pm 0.617$	$6.478 \pm 0.723$	$6.478 \pm 0.723$	$5.677 \pm 0.359$	$5.677 \pm 0.359$
$^{92}\text{Sr}$	2.71 h	1384.9	$90.0 \pm 0.3$	$6.005 \pm 0.479$	$6.017 \pm 0.480$	$5.258 \pm 0.199$	$5.259 \pm 0.199$	$5.248 \pm 0.569$	$5.259 \pm 0.570$
$^{93}\text{Y}$	10.18 h	266.9	$7.3 \pm 0.4$	$5.233 \pm 0.261$	$5.233 \pm 0.261$	$4.954 \pm 0.167$	$4.954 \pm 0.167$	$4.640 \pm 0.505$	$4.640 \pm 0.505$
$^{95}\text{Zr}$	64.02 d	724.2	$44.17 \pm 1.3$	$7.171 \pm 0.584$	$7.171 \pm 0.584$	$6.256 \pm 0.097$	$6.256 \pm 0.097$	$6.077 \pm 0.428$	$6.077 \pm 0.428$
$^{97}\text{Zr}$	16.91 h	743.4	$93.0 \pm 0.9$	$5.138 \pm 0.664$	$5.143 \pm 0.665$	$4.634 \pm 0.421$	$4.639 \pm 0.422$	$4.318 \pm 0.177$	$4.322 \pm 0.177$
$^{99}\text{Mo}$	65.94 h	140.5	$89.43 \pm 2.3$	$3.286 \pm 0.252$	$3.286 \pm 0.252$	$3.179 \pm 0.255$	$3.179 \pm 0.255$	$2.939 \pm 0.301$	$2.939 \pm 0.301$
		739.5	$12.13 \pm 1.2$	$3.305 \pm 0.299$	$3.305 \pm 0.299$	$3.244 \pm 0.292$	$3.244 \pm 0.292$	$3.303 \pm 0.296$	$3.303 \pm 0.296$
$^{103}\text{Ru}$	39.26 d	497.1	$90.9 \pm 1.0$	$0.620 \pm 0.062$	$0.622 \pm 0.062$	$0.656 \pm 0.083$	$0.622 \pm 0.083$	$0.969 \pm 0.164$	$0.969 \pm 0.164$
$^{105}\text{Rh}$	35.36 h	319.1	$19.0 \pm 1.0^{(a)}$	$0.218 \pm 0.019$	$0.218 \pm 0.019$	$0.366 \pm 0.051$	$0.366 \pm 0.051$	$0.446 \pm 0.041$	$0.466 \pm 0.041$
$^{112}\text{Ag}$	3.13 h	617.5	$43.0 \pm 2.2^{(a)}$	$0.266 \pm 0.033$	$0.266 \pm 0.033$	$0.477 \pm 0.037$	$0.477 \pm 0.037$	$0.623 \pm 0.150$	$0.624 \pm 0.150$
$^{115}\text{Cd}^{\text{g}}$	53.46 h	527.9	$27.45 \pm 1.8$	$0.237 \pm 0.024$		$0.417 \pm 0.083$		$0.562 \pm 0.102$	
$^{115}\text{Cd}^{\text{total}}$				$0.277 \pm 0.028^{(b)}$	$0.277 \pm 0.028^{(b)}$	$0.487 \pm 0.097^{(b)}$	$0.487 \pm 0.097^{(b)}$	$0.655 \pm 0.123^{(b)}$	$0.655 \pm 0.123^{(b)}$
$^{127}\text{Sb}$	3.85 d	685.7	$37.0 \pm 1.9^{(a)}$	$0.532 \pm 0.043$	$0.532 \pm 0.043$	$0.639 \pm 0.056$	$0.639 \pm 0.056$	$0.964 \pm 0.187$	$0.964 \pm 0.187$
$^{128}\text{Sn}$	59.07 min	482.3	$59.0 \pm 0.3$	$1.145 \pm 0.103$	$1.218 \pm 0.109$	$1.163 \pm 0.174$	$1.237 \pm 0.185$	$1.578 \pm 0.214$	$1.679 \pm 0.217$
$^{129}\text{Sb}$	4.32 h	812.8	$43.0 \pm 2.2^{(a)}$	$1.699 \pm 0.080$	$1.710 \pm 0.081$	$1.603 \pm 0.189$	$1.613 \pm 0.190$	$2.035 \pm 0.163$	$2.047 \pm 0.164$
$^{131}\text{I}$	8.02 d	364.5	$81.7 \pm 0.6$	$3.182 \pm 0.256$	$3.182 \pm 0.256$	$2.901 \pm 0.236$	$2.901 \pm 0.236$	$2.980 \pm 0.237$	$2.980 \pm 0.237$
$^{132}\text{Te}$	3.2 d	228.2	$88.0 \pm 1.8$	$4.136 \pm 0.304$	$4.136 \pm 0.304$	$3.815 \pm 0.345$	$3.846 \pm 0.348$	$3.416 \pm 0.232$	$3.440 \pm 0.234$
$^{133}\text{I}$	20.8 h	529.9	$87.0 \pm 1.7$	$5.598 \pm 0.394$	$5.603 \pm 0.394$	$5.166 \pm 0.412$	$5.172 \pm 0.412$	$5.013 \pm 0.301$	$5.018 \pm 0.302$
$^{134}\text{I}$	52.5 min	847.3	$95.4 \pm 0.3$	$6.569 \pm 0.588$	$6.582 \pm 0.589$	$6.692 \pm 0.412$	$6.705 \pm 0.412$	$6.615 \pm 0.817$	$6.628 \pm 0.819$
		884.1	$64.9 \pm 1.9$	$7.123 \pm 0.640$	$7.137 \pm 0.641$	$7.123 \pm 0.640$	$7.137 \pm 0.641$	$6.674 \pm 0.790$	$6.687 \pm 0.792$
$^{135}\text{I}$	6.57 h	1131.5	$22.7 \pm 1.4$	$4.927 \pm 0.301$	$4.977 \pm 0.304$	$5.822 \pm 0.528$	$5.881 \pm 0.533$	$5.147 \pm 0.621$	$5.199 \pm 0.628$
		1260.4	$28.9 \pm 1.7$	$5.157 \pm 0.155$	$5.209 \pm 0.157$	$5.244 \pm 0.523$	$5.297 \pm 0.528$	$5.174 \pm 0.554$	$5.227 \pm 0.560$
$^{139}\text{Ba}$	83.06 min	165.9	$23.7 \pm 2.4$	$7.465 \pm 0.556$	$7.465 \pm 0.556$	$7.197 \pm 0.343$	$7.197 \pm 0.343$	$6.892 \pm 0.732$	$6.892 \pm 0.732$
$^{140}\text{Ba}$	12.75 d	537.3	$24.4 \pm 0.7$	$8.358 \pm 0.551$	$8.358 \pm 0.551$	$8.299 \pm 0.579$	$8.299 \pm 0.579$	$7.579 \pm 0.491$	$7.579 \pm 0.491$
$^{141}\text{Ce}$	32.5 d	145.4	$48.2 \pm 0.3$	$7.304 \pm 0.423$	$7.304 \pm 0.423$	$6.983 \pm 0.598$	$6.893 \pm 0.598$	$6.811 \pm 0.828$	$6.811 \pm 0.828$
$^{142}\text{La}$	91.1 min	641.3	$47.0 \pm 2.0$	$6.383 \pm 0.551$	$6.383 \pm 0.551$	$6.265 \pm 0.403$	$6.265 \pm 0.403$	$6.251 \pm 0.851$	$6.251 \pm 0.851$
$^{143}\text{Ce}$	33.04 h	293.3	$42.8 \pm 1.3$	$6.777 \pm 0.399$	$6.777 \pm 0.399$	$6.780 \pm 0.459$	$6.780 \pm 0.459$	$6.669 \pm 0.741$	$6.669 \pm 0.741$
$^{147}\text{Nd}$	10.98 d	531.0	$13.1 \pm 0.7$	$2.197 \pm 0.019$	$2.203 \pm 0.019$	$2.412 \pm 0.134$	$2.419 \pm 0.134$	$2.118 \pm 0.313$	$2.124 \pm 0.314$
$^{150}\text{Pm}$	2.68 h	333.97	$68.0 \pm 3.4^{(a)}$	$0.502 \pm 0.104$	$0.503 \pm 0.104$	$0.472 \pm 0.055$	$0.473 \pm 0.056$	$0.528 \pm 0.051$	$0.529 \pm 0.051$

(a) Assumed value of 5%.

(b) The yields of  $^{115}\text{Cd}^{\text{total}}$  is based on the ratio of  $^{115}\text{Cd}^{\text{g}}/^{115}\text{Cd}^{\text{m}} = 6$  from ref. [71].

The absolute cumulative yields ( $Y_{\text{C}}$ ) of the fission products in the 6.35, 8.53 and 10.09 MeV neutron-induced fission of  $^{232}\text{Th}$  were then obtained from the mass-chain yield data and  $Y_{\text{FCY}}$  values by using eq. (7), which is the modified form of eq. (3),

$$Y_{\text{C}} = Y_{\text{A}} \times Y_{\text{FCY}}. \quad (7)$$

The absolute cumulative yield ( $Y_{\text{C}}$ ) and mass-chain yield ( $Y_{\text{A}}$ ) of the fission products in the 6.35, 8.53 and 10.09 MeV neutron-induced fission of  $^{232}\text{Th}$  along with the nuclear spectroscopic data from refs. [90,91] are given in table 1. The uncertainty shown in the measured cumulative yield of the individual fission products shown in table 1 is the statistical fluctuation of the mean value from two determinations. The overall uncertainty is the contributions from both random and systematic errors. The random error in the observed activity is due to counting statistics and is estimated to be 5–10%, which can be determined by accumulating the data for the optimum

period of time, depending on the half-life of the nuclide of interest. The overall systematic errors is about 3.8–10.5%, which comes from the uncertainties in irradiation time (0.2%), detector efficiency calibration ( $\sim 3\%$ ), half-life of the fission products ( $\sim 1\%$ ), and  $\gamma$ -ray intensity (2–10%) [90,91]. Thus for the yields of fission-products an upper limit of error of 6.3–34.7% was obtained based on 5–10% random error and a 3.8–10.5% systematic error.

## 4 Discussion

The fission products yields for  $^{232}\text{Th}(n, f)$  at average neutron energy of 8.53 and 10.09 MeV shown in table 1 are determined for the first time. At 6.35 MeV, the yields for  $^{232}\text{Th}(n, f)$  are the redetermined values and are in agreement with the literature data at 6.4 MeV [46]. The literature data [29–51] are based on mono-energetic neu-

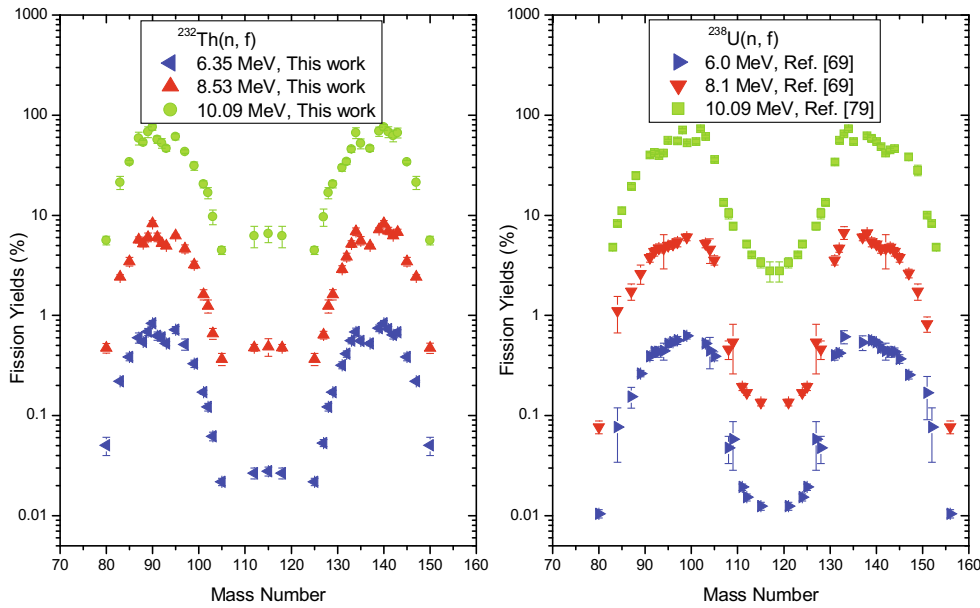


**Fig. 1.** Plot of the mass yields distribution in log scale from the quasi-mono-energetic neutron-induced fission of  $^{232}\text{Th}$  at 6.35, 8.53 and 10.09 MeV and of  $^{238}\text{U}$  at 6.0, 8.1 and 10.09 MeV.

trons, whereas the present data are for flux-weighted average neutron energies based on quasi-mono-energetic neutrons. The mass-chain yield data in  $^{232}\text{Th}(n, f)$  from the present work at average neutron energies of 6.35, 8.53 and 10.09 MeV are plotted as a function of their mass number in log and in linear scale in fig. 1 and fig. 2, respectively. In the same figures, the fission products yields in  $^{238}\text{U}(n, f)$  at neutron energies of 6.0, 8.1 and 10.09 MeV from the literature [70, 82] are also plotted for comparison. It can be seen, from fig. 1, that within the neutron energy of 6.4–10 MeV of present work, the mass-yield distribution in  $^{232}\text{Th}(n, f)$  is triple-humped, unlike in  $^{238}\text{U}(n, f)$ , where it is double-humped. The fission fragments yield distribution in the excitation energy range of the GDR region due to electromagnetic fission in inverse kinematics [22–24] for the neutron-deficient  $^{220-229}\text{Th}$  is also triple-humped and, for  $^{231-234}\text{U}$ , it is double-humped. This is due to the different type of potential energy surface in  $^{220-233}\text{Th}^*$  compared to  $^{231-239}\text{U}^*$  [93].

From fig. 2, it can be seen that both in  $^{232}\text{Th}(n, f)$  and  $^{238}\text{U}(n, f)$ , the yields of fission products for  $A = 133-134$ ,  $138-140$ ,  $143-144$  and their complementary products are higher than the other fission products. The oscillation of fission yields in the interval of five mass units around mass region of  $133-144$  is due to the even-odd effect [94]. The higher yields of fission products for  $A = 134-134$  and  $143-144$  can also be explained from the point of view of the standard I and standard II asymmetric fission modes as mentioned by Brossa *et al.* [95], which arise due to shell effects [96]. Based on standard I asymmetry, the fissioning system is characterized by spherical heavy fragment with mass numbers  $133-134$  due to the spherical  $82n$  shell and a deformed complementary light-mass fragment. Based on standard II asymmetry, the fissioning system is characterized by a deformed heavy-mass fragment near the mass

numbers of  $143-144$  due to a deformed  $86-88n$  shell and slightly deformed light-mass fragment. Thus, the higher yields of fission products for  $A = 133-134$  and  $143-144$  are due to the presence of spherical  $82n$  and deformed  $86-88n$  shells, respectively.

Further, it can be seen from fig. 2 that the yields of fission products for  $A = 133-134$  and  $143-144$  are lower than for  $A = 138-140$  in  $^{232}\text{Th}(n, f)$ . On the other hand, in  $^{238}\text{U}(n, f)$ , the yields of fission products for  $A = 133-134$  are higher than for  $A = 138-140$  and  $143-144$ . In order to examine this aspects, the yields of fission products for  $A = 133$ ,  $139$  and  $143$  from the present work (table 1) and literature data in the  $^{232}\text{Th}(n, f)$  [29–52] and  $^{238}\text{U}(n, f)$  [54–82] and are plotted in fig. 3 as a function of excitation energy. From fig. 3, it can be seen that at all excitation energy, the yields of fission products for  $A = 134$  and their complementary products are comparable in  $^{232}\text{Th}(n, f)$  and  $^{238}\text{U}(n, f)$ . On the other hand, the yields of fission products are higher marginally for  $A = 139$  and significantly for  $A = 143$  in  $^{232}\text{Th}(n, f)$  than in  $^{238}\text{U}(n, f)$ . This difference is based on the presence or absence of shells combination in the complementary pairs as explained in earlier work [82]. The variation of yields data for  $A = 133-134$ ,  $139-140$  and  $143-144$  in  $^{232}\text{Th}(n, f)$  and  $^{238}\text{U}(n, f)$  causes variation of the average heavy mass ( $\langle A_H \rangle$ ). In order to examine this, the average heavy mass ( $\langle A_H \rangle$ ) and light mass ( $\langle A_L \rangle$ ) in the  $^{232}\text{Th}(n, f)$  from the present work at average neutron energies of 6.35, 8.53 and 10.09 MeV as well as at other lower-neutron energies [29–52] were calculated from the mass-chain yields ( $Y_A$ ) of the fission products within the mass ranges of  $80-105$  and  $125-150$ , and by using the following relation:

$$\langle A_L \rangle = \frac{\sum (Y_A A_L)}{\sum Y_A}, \quad \langle A_H \rangle = \frac{\sum (Y_A A_H)}{\sum Y_A}. \quad (8)$$

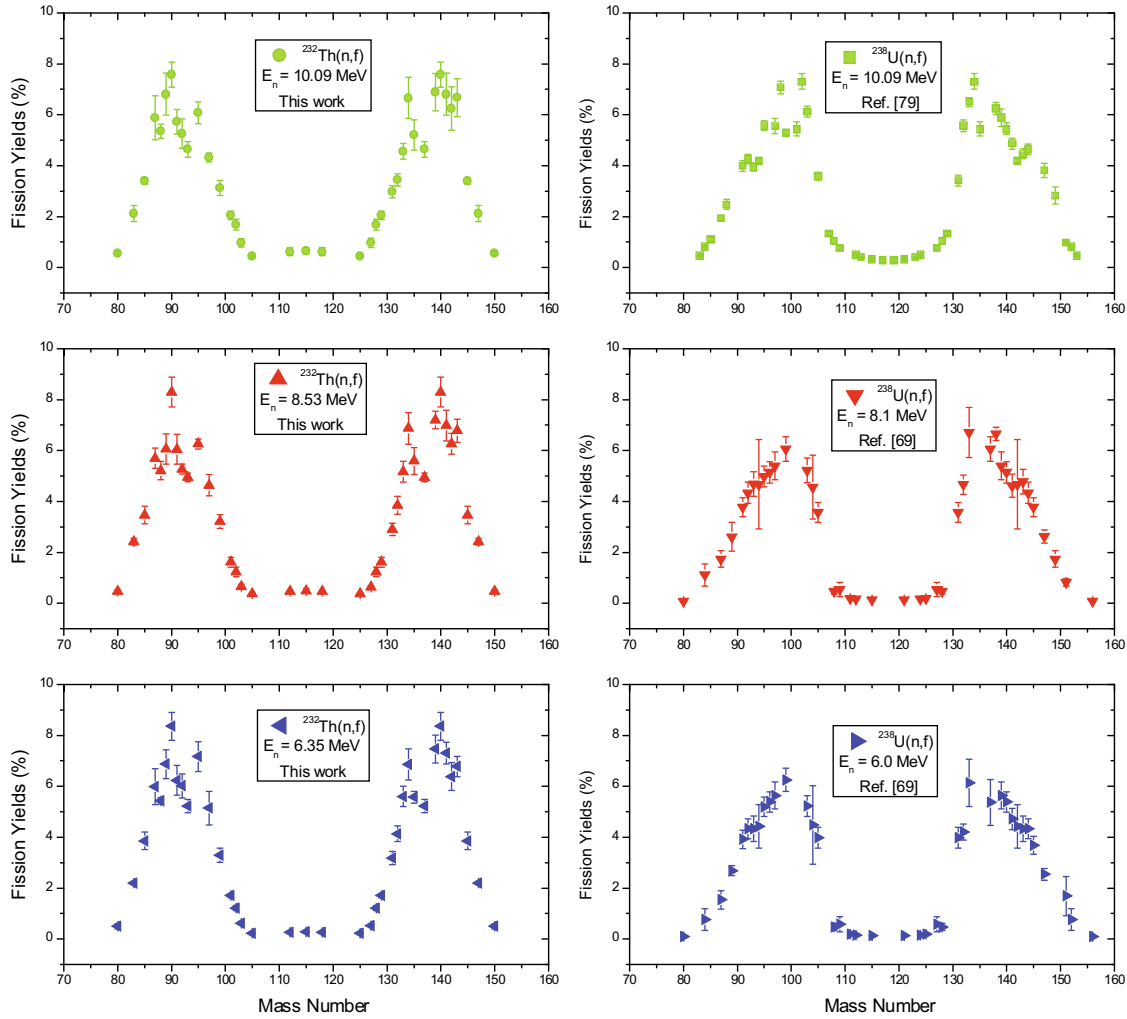


**Fig. 2.** Plot of the mass yields distribution in linear scale from the quasi-mono-energetic neutron-induced fission of  $^{232}\text{Th}$  at 6.35, 8.53 and 10.09 MeV and of  $^{238}\text{U}$  at 6.0, 8.1 and 10.09 MeV.

The  $\langle A_L \rangle$  and  $\langle A_H \rangle$  values obtained from the above relation in the  $^{232}\text{Th}(n, f)$  along with their corresponding average excitation energy ( $\langle E^* \rangle$ ) are given in table 2. The  $\langle A_L \rangle$  and  $\langle A_H \rangle$  values in the  $^{232}\text{Th}(n, f)$  from table 2 and literature data [54–82] in  $^{238}\text{U}(n, f)$  are plotted in fig. 4 as a function of excitation energy. It can be seen from fig. 4 that at all excitation energy, the  $\langle A_L \rangle$  values are significantly lower in  $^{232}\text{Th}(n, f)$  than in  $^{238}\text{U}(n, f)$ , whereas the  $\langle A_H \rangle$  values are higher in  $^{232}\text{Th}(n, f)$  than in  $^{238}\text{U}(n, f)$ . This is due to the favorable standard II asymmetric mode compared to standard I asymmetric mode of fission in  $^{232}\text{Th}(n, f)$  than in  $^{238}\text{U}(n, f)$ . However, significantly lower  $\langle A_L \rangle$  values in  $^{232}\text{Th}(n, f)$  than in  $^{238}\text{U}(n, f)$  are due to the mass conservation based on the standard I and II asymmetric mode of fission. It can be also seen from fig. 4 that the  $\langle A_H \rangle$  values for both  $^{232}\text{Th}(n, f)$  and  $^{238}\text{U}(n, f)$  reactions decrease with the excitation energy, whereas the  $\langle A_L \rangle$  values almost remain constant or slightly increase with the excitation energy. This is most probably due to the probability of more neutron emission from the heavy fragments [46].

**Table 2.** Average light mass ( $\langle A_L \rangle$ ), heavy mass ( $\langle A_H \rangle$ ) and average neutron numbers ( $\langle \nu \rangle_{\text{expt}}$ ) in the neutron-induced fission of  $^{232}\text{Th}$ .

$E_n$ (MeV)	$E^*$ (MeV)	$\langle A_L \rangle$	$\langle A_H \rangle$	$\langle \nu \rangle_{\text{expt}}$	Ref.
2.0	6.61	90.9	139.8	2.3	[46]
3.0	7.61	91.2	139.4	2.4	[46]
4.0	8.61	91.3	139.1	2.6	[46]
5.9	10.51	91.9	138.4	2.7	[46]
6.35	10.96	91.64	138.44	2.93	Present work
6.4	11.01	91.1	138.9	3.0	[46]
6.9	11.51	90.5	139.1	3.4	[46]
7.6	12.21	90.8	138.9	3.3	[46]
8.0	12.61	90.9	138.8	3.3	[46]
8.53	13.14	91.31	138.39	3.4	Present work
10.09	14.36	91.44	138.08	3.48	Present work
11.0	15.61	–	–	–	[30]
14.7	19.31	–	–	–	[50]
14.8	19.41	93.3	135.8	3.9	[31]

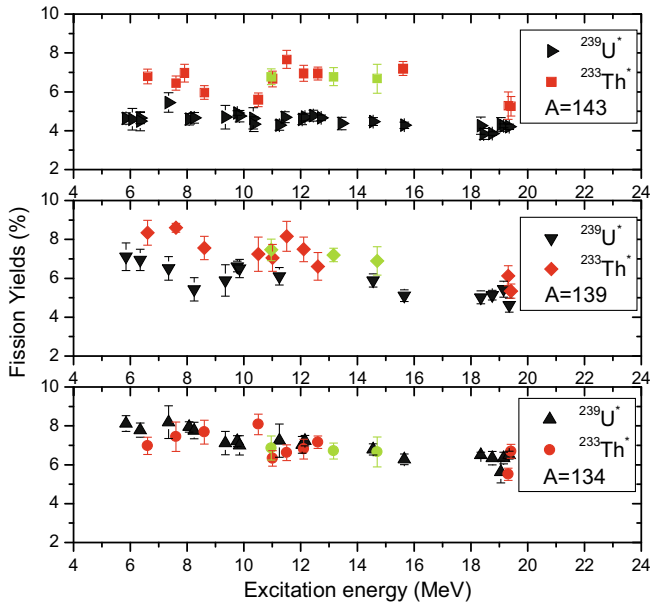


**Fig. 3.** Plot of yields of fission products (%) as a function of excitation energy for  $A = 143, 139$  and  $134$  in the  $^{232}\text{Th}(n, f)$  and  $^{238}\text{U}(n, f)$  reactions. The data of present work in  $^{232}\text{Th}(n, f)$  reaction are in green with the same symbol as the literature data.

From the  $\langle A_L \rangle$ ,  $\langle A_H \rangle$  and compound nucleus mass ( $A_C = 233$ ), the experimental average numbers of neutrons ( $\langle v \rangle_{\text{expt}}$ ) were calculated from the following relation:

$$\langle v \rangle_{\text{expt}} = A_C - (\langle A_L \rangle + \langle A_H \rangle). \quad (9)$$

The  $\langle v \rangle_{\text{expt}}$  values obtained from the above relation from the present work and literature data in  $^{232}\text{Th}(n, f)$  [29–52] at different excitation energies are also listed in table 2. The  $\langle v \rangle_{\text{expt}}$  values for  $^{232}\text{Th}(n, f)$  from table 2 and literature data [54–82] for  $^{238}\text{U}(n, f)$  are plotted in fig. 5 as a function of excitation energy. It can be seen from fig. 5 that in the neutron-induced fission of  $^{232}\text{Th}$  and  $^{238}\text{U}$ , the value of  $\langle v \rangle_{\text{expt}}$  increases with excitation energy. From fig. 5, it can also be seen that, at the same excitation energy, the  $\langle v \rangle_{\text{expt}}$  value in  $^{232}\text{Th}(n, f)$  is lower than in  $^{238}\text{U}(n, f)$ , which is due to the effect of fissility parameter besides excitation energy. However, at excitation energy around 11–13 MeV, the value of  $\langle v \rangle_{\text{expt}}$  in  $^{232}\text{Th}(n, f)$  is comparable or higher than in  $^{238}\text{U}(n, f)$ , which is due to GDR effect. Further, it can be seen from figs. 4 and 5 that the increasing trend of  $\langle v \rangle_{\text{expt}}$  and  $\langle A_L \rangle$  as well as decreasing trend of  $\langle A_H \rangle$  with excitation energy is not smooth in  $^{232}\text{Th}(n, f)$  as in the case of  $^{238}\text{U}(n, f)$ . Within excitation energy of 11–13 MeV, the increasing trend of  $\langle v \rangle_{\text{expt}}$  and  $\langle A_L \rangle$  as well as decreasing trend of  $\langle A_H \rangle$  with excitation energy is very sharp. This is due to major GDR effect in  $^{232}\text{Th}(n, f)$  compared to  $^{238}\text{U}(n, f)$  besides the effect of excitation energy.

The role of excitation energy on mass yield distribution at higher neutron energy fission of  $^{232}\text{Th}$  and  $^{238}\text{U}$  was clearly shown by I.V. Ryzhov *et al.* [53] from their data

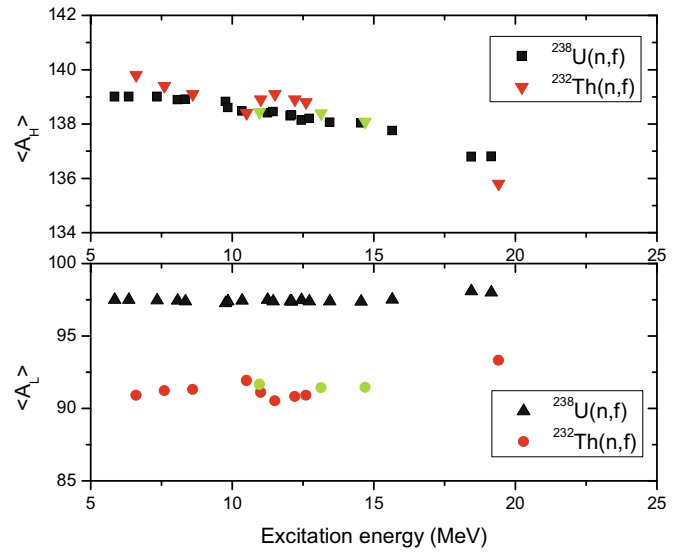


**Fig. 4.** Plot of average values of heavy mass ( $\langle A_H \rangle$ ) and average values of light mass ( $\langle A_L \rangle$ ) as a function of excitation energy in the  $^{232}\text{Th}(n, f)$  and  $^{238}\text{U}(n, f)$  reactions. The data of the present work in  $^{232}\text{Th}(n, f)$  reaction are in green with the same symbol as the literature data.

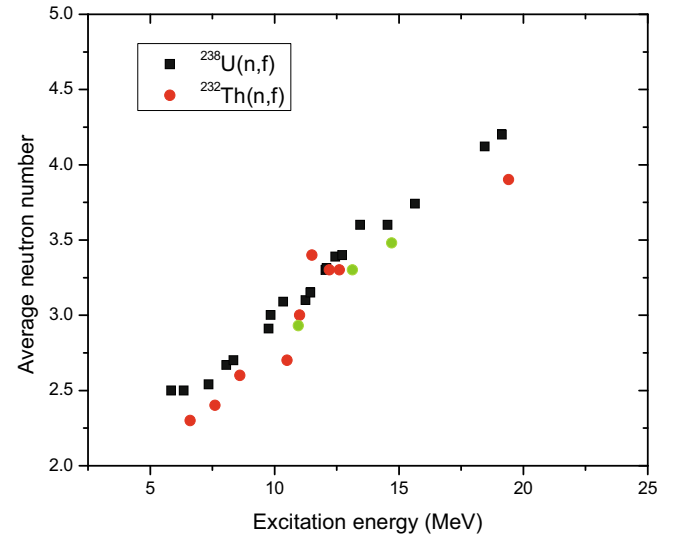


**Fig. 5.** Plot of yields of symmetric and asymmetric fission products (%) as a function of the excitation energy in the  $^{232}\text{Th}(n, f)$  and  $^{238}\text{U}(n, f)$  reactions. The data of the present work in the  $^{232}\text{Th}(n, f)$  reaction are in green with the same symbol as the literature data.

based on physical measurements. As mentioned by them at the same neutron energy, the symmetric fission is more enhanced in the case of  $^{232}\text{Th}(n, f)$  than in  $^{238}\text{U}(n, f)$ . In order to examine this aspect, the yields of symmetric products, high yield asymmetric products and the peak-to-valley ( $P/V$ ) ratios from the present work and literature data [29–52] in  $^{232}\text{Th}(n, f)$  are shown in table 3.

**Table 3.** Yields of asymmetric ( $Y_a$ ) and symmetric ( $Y_s$ ) products and the  $P/V$  ratio in the neutron-induced fission of  $^{232}\text{Th}$ .

$E_n$ (MeV)	$E^*$ (MeV)	$Y_a$ (%)	$Y_s$ (%)	$P/V$ ratio	Ref.
$1.60 \pm 0.02$	6.21	–	–	$218.9 \pm 47.7$	[45]
$1.68 \pm 0.02$	6.29	–	–	$205.1 \pm 42.1$	[45]
$1.72 \pm 0.02$	6.33	–	–	$292.7 \pm 73.2$	[45]
$1.77 \pm 0.02$	6.38	–	–	$241.5 \pm 58.8$	[45]
$1.88 \pm 0.02$	6.49	–	–	$238.2 \pm 36.5$	[45]
$2.00 \pm 0.02$	6.61	–	–	$283.5 \pm 64.9$	[45]
2.00	6.61	$8.950 \pm 0.250$	$0.005 \pm 0.001$	–	[46]
$2.20 \pm 0.02$	6.81	–	–	$212.3 \pm 53.9$	[45]
$2.43 \pm 0.02$	7.04	–	–	$214.5 \pm 35.6$	[45]
$2.96 \pm 0.41$	7.57	–	–	$118.5 \pm 17.5$	[45]
2.97	7.58	–	–	122.0	[41]
3.00	7.61	$8.600 \pm 0.230$	$0.023 \pm 0.004$	–	[46]
3.00	7.61	$7.890 \pm 0.094$	$0.045 \pm 0.009$	–	[31]
$3.10 \pm 0.15$	7.71	–	–	$63.0 \pm 11.0$	[47]
4.00	8.61	$8.010 \pm 0.200$	$0.099 \pm 0.015$	$80.9 \pm 12.3$	[46]
$4.03 \pm 0.02$	8.64	–	–	71.0	[41]
$4.20 \pm 0.11$	8.81	–	–	$27.2 \pm 3.1$	[45]
$4.81 \pm 0.02$	9.52	–	–	51.0	[41]
$5.20 \pm 0.25$	9.87	–	–	$29.0 \pm 3.0$	[47]
$5.30 \pm 0.11$	9.91	–	–	$26.4 \pm 2.1$	[45]
5.90	10.51	$8.080 \pm 0.530$	$0.270 \pm 0.040$	$29.9 \pm 4.8$	[46]
6.35	10.96	$8.358 \pm 0.551$	$0.277 \pm 0.028$	$30.3 \pm 4.4$	Present work
6.40	11.01	$8.410 \pm 0.630$	$0.230 \pm 0.040$	$36.6 \pm 6.9$	[46]
6.90	11.51	$8.700 \pm 0.340$	$0.200 \pm 0.030$	$43.5 \pm 6.7$	[46]
7.60	12.21	$8.380 \pm 0.230$	$0.200 \pm 0.030$	$41.9 \pm 6.4$	[46]
8.00	12.61	$7.870 \pm 0.350$	$0.290 \pm 0.030$	$27.1 \pm 3.9$	[46]
8.53	13.14	$8.299 \pm 0.579$	$0.487 \pm 0.097$	$17.1 \pm 3.6$	Present work
$9.10 \pm 0.30$	13.71	$(8.000 \pm 0.500)$	$0.436 \pm 0.014$	$18.3 \pm 1.3$	[32]
10.09	14.70	$7.579 \pm 0.491$	$0.655 \pm 0.123$	$11.6 \pm 2.6$	Present work
11.00	15.61	$8.100 \pm 0.900$	$0.760 \pm 0.015$	$10.7 \pm 1.3$	[30]
$13.40 \pm 0.17$	18.01	$(8.000 \pm 0.500)$	$1.440 \pm 0.020$	$5.60 \pm 0.36$	[32]
$14.10 \pm 0.16$	18.71	$(7.500 \pm 0.500)$	$1.340 \pm 0.020$	$5.60 \pm 0.38$	[32]
$14.70 \pm 0.30$	19.31	$(7.500 \pm 0.500)$	$1.580 \pm 0.050$	$4.75 \pm 0.51$	[50]
$14.70 \pm 0.30$	19.31	–	$1.400 \pm 0.050$	$5.36 \pm 0.41$	[50]
$14.70 \pm 0.30$	19.31	–	$1.310 \pm 0.140$	$5.73 \pm 0.72$	[38]
$14.70 \pm 0.30$	19.31	–	$1.380 \pm 0.120$	$5.43 \pm 0.59$	[48]
$14.80 \pm 0.80$	19.41	$6.690 \pm 0.325$	$1.720 \pm 0.500$	$3.89 \pm 1.15$	[31]
$14.80 \pm 0.80$	19.41	–	$1.500 \pm 0.200$	$4.46 \pm 0.65$	[34]
$14.80 \pm 0.80$	19.41	–	$1.240 \pm 0.200$	$5.40 \pm 0.92$	[33]
$14.90 \pm 0.25$	19.51	$(6.500 \pm 0.500)$	$1.280 \pm 0.040$	$5.10 \pm 0.42$	[32]
$18.10 \pm 0.25$	22.71	$(6.500 \pm 0.500)$	$1.920 \pm 0.100$	$3.40 \pm 0.31$	[32]

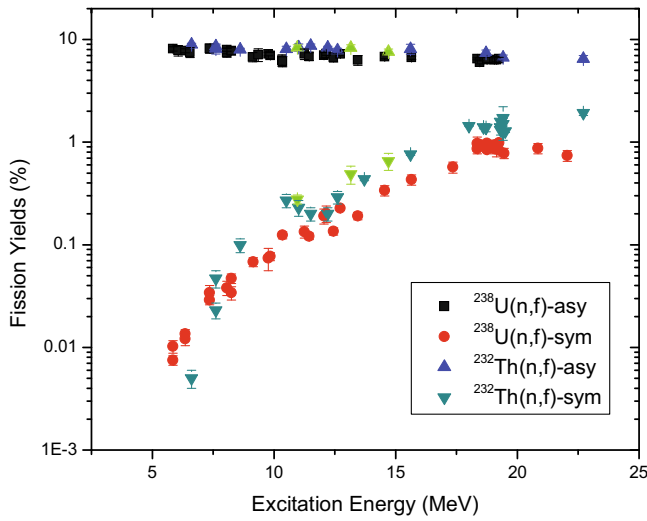


**Fig. 6.** Plot of the peak-to-valley ( $P/V$ ) ratio as a function of the excitation energy in the  $^{232}\text{Th}(n, f)$  and  $^{238}\text{U}(n, f)$  reactions. The data of present work in  $^{232}\text{Th}(n, f)$  are in green with the same symbol as the literature data.

The yields of high-yield fission products and symmetric products from table 3 in  $^{232}\text{Th}(n, f)$  and similar data from the literature [54–82] in  $^{238}\text{U}(n, f)$  are plotted in fig. 6 as a function of excitation energy. It can be seen from fig. 6 that in both  $^{232}\text{Th}(n, f)$  and  $^{238}\text{U}(n, f)$ , the yields of asymmetric products decrease slightly, whereas the yields of symmetric products increase significantly with excitation energy. It can be also seen from fig. 6 that the yields of symmetric products in  $^{232}\text{Th}(n, f)$  increase sharply up to excitation energy of 10 MeV and then slightly decrease up to 13 MeV and thereafter again increase. On the other hand, in  $^{238}\text{U}(n, f)$ , the increase of yields of symmetric products is nearly smooth with excitation energy. The different behavior of  $^{232}\text{Th}(n, f)$  compared to  $^{238}\text{U}(n, f)$  within excitation energy of 10–12.5 MeV is due to the greater effect of giant dipole resonance (GDR) in the former than in the later. Similar effect within excitation energy of 10–13 MeV was also seen in the proton-induced fission of  $^{232}\text{Th}$  [97], which supports the present observation. Otherwise, above excitation energy of 7.5 MeV, the yields of symmetric products are higher in  $^{232}\text{Th}(n, f)$  than in  $^{238}\text{U}(n, f)$  and increase with excitation energy. The role of excitation energy can be also from the peak-to-valley ( $P/V$ ) ratio. Thus from table 3, the  $P/V$  ratios in  $^{232}\text{Th}(n, f)$  and similar data from the literature [54–82] in  $^{238}\text{U}(n, f)$  are plotted in fig. 7 as a function of excitation energy. It can be seen from fig. 7 that in both  $^{232}\text{Th}(n, f)$  and  $^{238}\text{U}(n, f)$ , the  $P/V$  decreases with excitation energy. However, the  $P/V$  ratio in  $^{232}\text{Th}(n, f)$  decreases up to 10 MeV and then slightly increases up to 13 MeV and thereafter again decrease, which is due to the GDR effect. It can also be seen from fig. 7 that at all excitation energy, the  $P/V$  ratio in  $^{232}\text{Th}(n, f)$  is lower than in  $^{238}\text{U}(n, f)$ . This is due to the different type of potential energy surface in  $^{233}\text{Th}^*$  compared to  $^{239}\text{U}^*$  [93] as mentioned before besides the role of excitation energy.

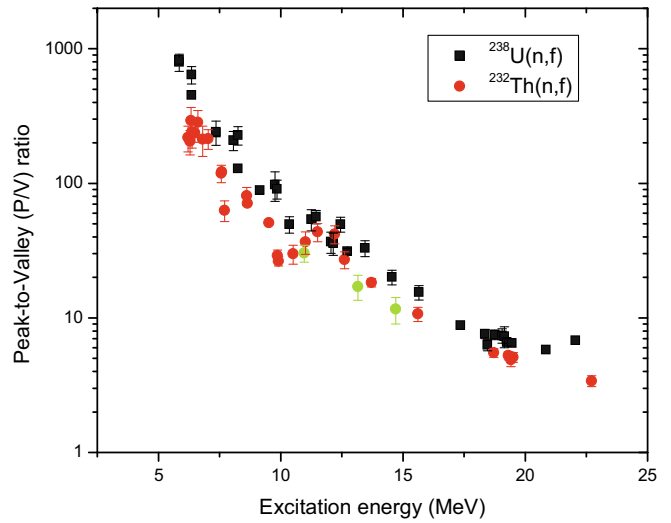


**Fig. 7.** Plot of the average neutron number ( $\langle v \rangle$ ) as a function of the excitation energy in the  $^{232}\text{Th}(n, f)$  and  $^{238}\text{U}(n, f)$  reactions. The data of the present work in  $^{232}\text{Th}(n, f)$  are in green with the same symbol as the literature data.

## 5 Conclusions

- i) The yields of fission products in the 6.35, 8.53 and 10.09 MeV quasi-neutron-induced fission of  $^{232}\text{Th}$  were determined by using an off-line  $\gamma$ -ray spectrometric technique. From the yields of various products mass-chain yields were obtained by using charge distribution corrections.
- ii) In the average neutron energy of 6.35, 8.53 and 10.09 MeV, the mass-yield distributions in the  $^{232}\text{Th}(n, f)$  is triple-humped unlike in  $^{238}\text{U}(n, f)$ , where it is double-humped. This is due to the different type of potential energy surface in  $^{233}\text{Th}^*$  than in  $^{239}\text{U}^*$ .
- iii) The yields of fission products for  $A = 133$ – $134$ ,  $A = 138$ – $140$ , and  $A = 143$ – $144$  and their complementary products are higher than those of other fission products for  $^{232}\text{Th}(n, f)$  and  $^{238}\text{U}(n, f)$  reactions. This is due to shell closure proximity based on standard I and II asymmetric mode of fission besides the role of even-odd effect.
- iv) In  $^{232}\text{Th}(n, f)$  and  $^{238}\text{U}(n, f)$ , the  $\langle v \rangle$  and  $\langle A_L \rangle$  values increase and  $\langle A_H \rangle$  values decrease with excitation energies. However, within the excitation energy of 10–13 MeV, the increasing trends of  $\langle v \rangle$  and  $\langle A_L \rangle$  and the decreasing trend of  $\langle A_H \rangle$  with excitation energy is sharp in  $^{232}\text{Th}(n, f)$  reaction. This is due to the major GDR effect in the  $^{232}\text{Th}(n, f)$  reaction than in the  $^{238}\text{U}(n, f)$  reaction.
- v) In  $^{232}\text{Th}(n, f)$  and  $^{238}\text{U}(n, f)$ , the yields of high-yield asymmetric products decrease marginally, whereas for symmetric products increase sharply with excitation energies. In  $^{238}\text{U}(n, f)$  reaction, the yields of symmetric fission products increase smoothly with excitation energy. However, in  $^{232}\text{Th}(n, f)$ , the yields of symmetric

products increase sharply within excitation energy of 10 MeV and then decreases up to 12.5 MeV and thereafter again increase with excitation energy.

- vi) The  $P/V$  ratios in  $^{232}\text{Th}(n, f)$  and  $^{238}\text{U}(n, f)$  decrease with excitation energy. This shows the role of excitation energy. However, at all excitation energies, the  $P/V$  ratio in the  $^{232}\text{Th}(n, f)$  are lower than in the  $^{238}\text{U}(n, f)$ , which is due to the different type of potential surface between two fissioning systems.

## References

- S.F. Mughabghab, M. Diveenam, N.E. Holden, *Neutron Resonance Parameters and Thermal Cross Sections*, Vol. I (Academic Press, New York, 1981).
- R. Vandenbosch, J.R. Huizenga, *Nuclear Fission* (Academic, New York, 1973).
- C. Wagemans, *The Nuclear Fission Process* (CRC, London, 1990).
- E.A.C. Crouch, *At. Data Nucl. Data Tables* **19**, 417 (1977).
- B.F. Rider, *Compilation of fission products yields*, NEDO, 12154 3c ENDF-327, Valeciceitos Nuclear Centre (1981).
- J.R. England, B.F. Rider, *Evaluation and compilation of fission products yields*, ENDF/BVI (1989, 1992).
- M. James, R. Mills, *Neutron fission products yields*, UKFY2 (1991) and JEF-2.2 (1993).
- A.C. Wahl, *At. Data Nucl. Data Tables* **39**, 1 (1988).
- Fast Reactors and Accelerator Driven Systems Knowledge Base, IAEA-TECDOC-1319: *Thorium fuel utilization: Options and Trends*.
- L. Mathieu *et al.*, *Proportion for a very simple Thorium Molten Salt reactor*, in *Proceedings of the Global International Conference*, Paper No. 428 (Tsukuba, Japan, 2005).
- A. Nuttin, D. Heuer, A. Bilibaud, R. Brissot, C. Le Brun, E. Liatard, J.M. Loiseaux, L. Mathieu, O. Meplan, E. Merle-Lucotte, H. Nifenecker, F. Perdu, S. David, *Proc. Nucl. Energy* **46**, 77 (2005).
- T.R. Allen, D.C. Crawford, *Sci. Technol. Nucl. Install.* **2007**, 97486 (2007).
- Annual Project Status Report 2000, MIT-ANP-PR-071, INEFL/EXT-2009-00994.
- R.K. Sinha, A. Kakodkar, *Nucl. Eng. Des.* **236**, 683 (2006).
- S. Ganesan, *Creation of Indian experimental benchmarks for thorium fuel cycle*, IAEA Coordinated research project on "Evaluated data for thorium-uranium fuel cycle", in *Third Research Co-ordination Meeting, 30 January to 2 February 2006, Vienna, Austria*, INDC (NDS)-0494 (2006).
- F. Carminati, R. Klapisch, J.P. Revol, J.A. Rubia, C. Rubia, *CERN/AT/93-49 (ET)* 1993.
- C. Rubia, J.A. Rubio, S. Buono, F. Carminati, N. Fietier, J. Galvez, C. Geles, Y. Kadi, R. Klapisch, P. Mandrillon, J.P. Revol, Ch. Roche, *CERN/AT/95-44 (ET)* 1995, *CERN/AT/95-53(ET)* 1995, *CERN/LHC/96-01 (LET)* 1996, *CERN/LHC/97-01 (EET)* 1997.
- C.D. Bowman, *AIP Conf. Proc.* **346**, 22 (1994).
- Accelerator Driven Systems: Energy Generation and Transmutation of Nuclear Waste, Status report, IAEA, Vienna, IAEA-TECDO-985, Nov. 1997.
- C.D. Bowman, *Annu. Rev. Nucl. Part Sci.* **48**, 505 (1998).
- S. Ganesan, *Pramana J. Phys.* **68**, 257 (2007).
- K.-H. Schmidt, S. Steinhauser, C. Bockstiegel, A. Rewe, A. Heinz, A.R. Junghans, J. Benlliure, H.-G. Clerc, M. de Jong, J. Muller, M. Pfutzner, B. Voss, *Nucl. Phys. A* **665**, 221 (2000).
- S. Steinhauser, J. Benlliure, C. Bockstiegel, H.-G. Clerc, A. Heinz, A. Rewe, M. de Jong, A.R. Junghans, J. Muller, M. Pfutzner, K.-H. Schmidt, *Nucl. Phys. A* **634**, 89 (1998).
- J. Benlliure, A.R. Junghans, K.-H. Schmidt, *Eur. Phys. J. A* **13**, 93 (2002).
- R.H. Iyer, C.K. Mathews, N. Ravindran, K. Rengan, D.V. Singh, M.V. Ramaniah, H.D. Sharma, *J. Inorg. Nucl. Chem.* **25**, 465 (1963).
- H.N. Erten, A. Grutter, E. Rossler, H.R. von Gunten, *Nucl. Sci. Eng.* **79**, 167 (1981).
- H. Naik, A.G.C. Nair, P.C. Kalsi, A.K. Pandey, R.J. Singh, A. Ramaswami, R.H. Iyer, *Radiochim. Acta* **75**, 69 (1996).
- R.H. Iyer, H. Naik, A.K. Pandey, P.C. Kalsi, R.J. Singh, A. Ramaswami, A.G.C. Nair, *Nucl. Sci. Eng.* **135**, 227 (2000).
- A. Turkevich, J.B. Niday, *Phys. Rev.* **84**, 52 (1951).
- A. Turkevich, J.B. Niday, A. Tompkins, *Phys. Rev.* **89**, 552 (1953).
- K.M. Broom, *Phys. Rev. B* **133**, 874 (1964).
- G.P. Ford, R.B. Leachman, *Phys. Rev. B* **137**, 826 (1965).
- R. Ganapathy, P.K. Kuroda, *J. Inorg. Nucl. Chem.* **28**, 2071 (1966).
- Tin Mo, M.N. Rao, *J. Inorg. Nucl. Chem.* **30**, 345 (1968).
- M. Thin, M.N. Rao, P.K. Kurdo, *J. Inorg. Nucl. Chem.* **30**, 1145 (1968).
- A.I. Sagachev, V.G. Vorobeieva, B.D. Kuzminov, V.B. Mikhaylov, Z. Tarsko, *Sov. J. Nucl. Phys.* **7**, 475 (1968).
- S.J. Lyle, J. Sellaers, *Radiochim. Acta* **12**, 43 (1969).
- L.H. Gevaert, R.E. Jervis, H.D. Sharma, *Can. J. Chem.* **48**, 641 (1970).
- J. Blachot, L.C. Carraz, P. Cavallini, E. Monnard, F. Schusslor, *J. Radioanal. Nucl. Chem.* **7**, 309 (1971).
- D.L. Swindle, D.T. Moore, J.N. Beck, P.K. Kuroda, *J. Inorg. Nucl. Chem.* **33**, 3643 (1971).
- W. Holubarsch, L. Pfeiffer, F. Gonnenswein, *Nucl. Phys. A* **171**, 631 (1971).
- S.A. Rao, *Phys. Rev.* **5**, 171 (1972).
- J.P. Bocquet, R. Brissot, J. Crancon, A. Moussa, *Nucl. Phys. A* **189**, 556 (1972).
- S.M. Dubroviva, V.I. Nogorodtseva, L.N. Morozov, V.A. Pchevin, L.V. Chistyakov, V.A. Schigin, V.M. Shubko, *Yad. Fiz.* **17**, 1470 (1973).
- J. Trochon, H.A. Yehia, F. Brisard, Y. Pranal, *Nucl. Phys. A* **318**, 63 (1979).
- L.E. Glendenin, J.E. Gindler, I. Ahmad, D.J. Henderson, J.W. Meadows, *Phys. Rev. C* **22**, 152 (1980).
- S.T. Lam, L.L. Yu, H.W. Fielding, W.K. Dawson, G.C. Neilson, *Phys. Rev. C* **28**, 1212 (1983).
- A.E. Richoortson, H.L. Wright, J.L. Meason, J.R. Smith, *Nucl. Sci. Eng.* **94**, 413 (1986).
- Li Wen-Xin, Sun Tong-Yu, Sun Xiu-Hua, Fu Min, Dong Tian-Rong, Zheng Man-Jiao, *High Energy Phys. Nucl. Phys.* **11**, 376 (1987).
- Sun Tong-Yu, Li Wen-Xin, Dong Tian-Rong, Fu Min, *High Energy Phys. Nucl. Phys.* **12**, 221 (1988).
- V.D. Simutkin, I.V. Ryzhov, G.A. Tutin, L.A. Vaishnena, J. Blongren, S. Pomp, M. Oesterlung, P. Andersson, R. Bevilacqua, J.P. Menlders, R. Prieels, *AIP Conf. Proc.* **1175**, 393 (2010).

52. P.M. Prajapati, H. Naik, S. Mukherjee, S.V. Suryanarayana, B.S. Shivashankar, R. Crasta, V.K. Mulik, K.C. Jagadeesan, S.V. Thakre, A. Goswami, Nucl. Sci. Eng. **176**, 1 (2014).
53. I.V. Ryzhov, S.G. Yavshits, G.A. Tutin, N.V. Kovalev, A.V. Saulski, N.A. Kudryashev, A.V. Saulski, N.A. Kudryashev, M.S. Onegin, L.A. Vaishnene, Yu.A. Gavrikov, O.T. Grudzevich, V.D. Simutkin, S. Pomp, J. Blomgren, M. Osterlund, P. Andersson, R. Bevilacqua, J. Meulders, R. Prieels, Phys. Rev. C **83**, 054603 (2011).
54. K.M. Brown, Phys. Rev. **126**, 627 (1962).
55. M.P. Menon, P.K. Kurdo, J. Inorg. Nucl. Chem. **26**, 40 (1964).
56. N.L. Borisova, S.M. Dubrovina, V.I. Novgorodtseva, V.A. Pchelina, V.A. Shigin, V.M. Shubko, Sov. J. Nucl. Phys. **6**, 331 (1968).
57. S.J. Lyle, J. Tillars, Radiochim. Acta **12**, 43 (1969).
58. D.J. Gorman, R.H. Tomilson, Can. J. Chem. **46**, 1663 (1968).
59. S.J. Lyle, J. Sellier, Radiochim. Acta **12**, 43 (1968).
60. S.J. Lyle, R. Wellum, Radiochim. Acta **13**, 167 (1969).
61. S.G. Birgul, S.J. Lyle, R. Wellum, Radiochim. Acta **16**, 104 (1971).
62. J.P. Bocquet, Nucl. Phys. **189**, 556 (1972).
63. D.R. Nethaway, B. Mendoza, Phys. Rev. C **6**, 1821 (1972).
64. D.R. Nethaway, B. Mendoza, Phys. Rev. C **6**, 1827 (1972).
65. J. Blachot, L.C. Carraz, P. Cavalini, C. Chauvin, A. Ferrieu, A. Moussa, J. Inorg. Nucl. Chem. **36**, 495 (1974).
66. J.T. Harvey, D.E. Adams, W.D. James, J.N. Beck, J.L. Meason, P.K. Kuroda, J. Inorg. Nucl. Chem. **37**, 2243 (1975).
67. D.E. Adams, W.D. James, J.N. Beck, P.K. Kuroda, J. Inorg. Nucl. Chem. **37**, 419 (1975).
68. M. Rajagopalan, H.S. Pruys, A. Grutter, E.A. Hermes, H.R. von Gunten, J. Inorg. Nucl. Chem. **38**, 351 (1976).
69. S. Daroczy, P. Raics, S. Nagy, L. Koever, I. Hamvas, E. Gorman, ATOMKI Kozl. **18**, 317 (1976).
70. T.C. Chapman, G.A. Anzelon, G.C. Spitale, D.R. Nethaway, Phys. Rev. C **17**, 1089 (1978).
71. S. Nagy, K.F. Flynn, J.E. Gindler, J.W. Meadows, L.E. Glendenin, Phys. Rev. C **17**, 163 (1978).
72. L. We-Xin, S. Tong-Yu, Z. Man-Jiao, D. Tian-Rong, S. Xiu-Hua, He Hua-Xue, Yu F. Hua-Kue, High Energy Phys. Nucl. Phys. **2**, 9 (1980).
73. L. We-Xin, S. Tong-Yu, Z. Man-Jiao, D. Tian-Rong, S. Xiu-Hua, He Hua-Xue, Yu F. Hua-Kue, High Energy Phys. Nucl. Phys. **5**, 176 (1983).
74. L. Ze, Z. Chun-Hua, L. Cong-Gui, W. Xiu-Zhi, Q. Lim-Kun, C. Anzhi, L. Hui-Jung, Z. Su-Jing, L. Yong-Hui, Ju Chang-Xin, L. Da-Ming, T. Pei-Ja, M. Jiang-Chen, J. Ki-Xing, High Energy Phys. J. Nucl. Phys. **7**, 97 (1985).
75. L. Cong-Gui, L. Hui-Jun, L. Yong-Hui, High Energy Phys. Nucl. Phys. **7**, 235 (1985).
76. A. Afarideh, K.R. Annole, Ann. Nucl. Energy **16**, 313 (1989).
77. Z. Li, X. Wang, K. Jing, A. Cui, D. Liu, S. Su, P. Tang, T. Chih, S. Zhang, J. Gao, Radiochim. Acta **64**, 95 (1994).
78. G. Lhersonnau, P. Denloov, G. Canchel, J. Huikari, J. Jardin, A. Tokinen, V. KOLhinen, C. Lau, L. Lebroton, A.C. Mueller, A. Nieminen, S. Nummela, H. Penttila, K. Perajavi, Z. Radivojevic, V. Rubchenya, M.G. Saint-Laurent, W.H. Trzaska, D. Vakhtin, J. Vervier, A.C. Villari, J.C. Viang, J. Aystoe, Eur. Phys. J. A **9**, 385 (2000).
79. I. Clenk, Radiochim. Acta **85**, 85 (1999).
80. I. Clenk, Radiochim. Acta **89**, 481 (2001).
81. J. Laurec, A. Adam, T. DeBruyne, E. Brauge, T. Granier, J. Aupiais, O. Barsillon, G. Lepetit, N. Authier, P. Casoli, Nucl. Data Sheet **111**, 2965 (2010).
82. H. Naik, V.K. Mulik, P.M. Prajapati, B.S. Shivasankar, S.V. Suryanarayana, K.C. Jagadeesan, S.V. Thakre, S.C. Sharma, A. Goswami, Nucl. Phys. A **913**, 185 (2013).
83. H. Umezawa, S. Baba, H. Baba, Nucl. Phys. A **160**, 65 (1971).
84. P.M. Prajapati, H. Naik, S.V. Suryanarayana, S. Mukherjee, K.C. Jagadeesan, S.C. Sharma, S.V. Thakre, K.K. Rasheed, S. Ganesan, A. Goswami, Eur. Phys. J. A **48**, 35 (2012).
85. R. Crasta, H. Naik, S.V. Suryanarayana, B.S. Shivashankar, V.K. Mulik, P.M. Prajapati, Ganesh Sanjeev, S.C. Sharma, P.V. Bhagwat, A.K. Mohanty, S. Ganesan, A. Goswami, Ann. Nucl. Energy **47**, 160 (2012).
86. J.F. Ziegler, J.P. Biersack, U. Littmark, *SRIM 2003 code. The stopping and Range of Ions in Solids* (Pergamon, New York, 2003).
87. H. Liskien, A. Paulsen, At. Data Nucl. Data Tables **15**, 57 (1975).
88. J.W. Meadows, D.L. Smith, *Neutrons from proton bombardment of natural Lithium*, Argonne National Laboratory Report ANL-7983 (1972).
89. C.H. Poppe, J.D. Anderson, J.C. Davis, S.M. Grimes, C. Wong, Phys. Rev. C **14**, 438 (1976).
90. E. Browne, R.B. Firestone, in *Table of Radioactive Isotopes*, edited by V.S. Shirley (Wiley, New York, 1986) and R.B. Firestone, L.P. Ekstrom, in *Table of Radioactive Isotopes*, Version 2.1 (2004) <http://ie.lbl.gov/toi/index.asp>.
91. J. Blachot, C. Fiche, Ann. Phys. Suppl. **6**, 3 (1981).
92. N. Sugarman, A. Turkevich, in *Radiochemical Studies: The Fission Product*, edited by C.D. Coryell, N. Sugarman, Vol. **3** (McGraw-Hill, New York, 1951) p. 1396.
93. P. Moller, Nucl. Phys. A **192**, 529 (1972).
94. H. Naik, R.J. Singh, R.H. Iyer, Eur. Phys. J. A **16**, 495 (2003).
95. U. Brossa, S. Grossmann, A. Muller, Phys. Rep. **197**, 167 (1990).
96. B.D. Wilkins, E.P. Steinberg, R.R. Chasman, Phys. Rev. C **14**, 1832 (1976).
97. H. Kudo, H. Muramatsu, H. Nakahara, K. Miyano, I. Kohno, Phys. Rev. C **25**, 3011 (1982).